Designing novel thin film polycrystalline solar cells for high efficiency: sandwich CIGS and heterojunction perovskite*

Tianyue Wang[1], Jiewei Chen[1], Gaoxiang Wu[1], Dandan Song[1], and Meicheng Li[1, 2, †]

[1]State Key Laboratory of Alternate Electrical Power System with Renewable Energy Sources, North China Electric Power University, Beijing 102206, China
[2]Chongqing Materials Research Institute, Chongqing 400707, China

Abstract: Heterojunction and sandwich architectures are two new-type structures with great potential for solar cells. Specifically, the heterojunction structure possesses the advantages of efficient charge separation but suffers from band offset and large interface recombination; the sandwich configuration is favorable for transferring carriers but requires complex fabrication process. Here, we have designed two thin-film polycrystalline solar cells with novel structures: sandwich CIGS and heterojunction perovskite, referring to the advantages of the architectures of sandwich perovskite (standard) and heterojunction CIGS (standard) solar cells, respectively. A reliable simulation software wxAMPS is used to investigate their inherent characteristics with variation of the thickness and doping density of absorber layer. The results reveal that sandwich CIGS solar cell is able to exhibit an optimized efficiency of 20.7%, which is much higher than the standard heterojunction CIGS structure (18.48%). The heterojunction perovskite solar cell can be more efficient employing thick and doped perovskite films (16.9%) than these typically utilizing thin and weak-doping/intrinsic perovskite films (9.6%). This concept of structure modulation proves to be useful and can be applicable for other solar cells.

Key words: sandwich CIGS solar cell; heterojunction perovskite solar cell; simulation; wxAMPS
DOI: 10.1088/1674-4926/38/1/014005 **PACS:** 82.20.Wt; 88.40.H-; 78.56.-a

1. Introduction

In solar cells, heterojunction and sandwich architectures are two kinds of promising structure configurations that have been widely applied for designing efficient devices[1−3]. Specifically, the heterojunction structure is fabricated by stacking up two different semiconductor materials together with different doping to control the conduction type, i.e. the n-type and p-type. Therefore, the typical heterojunction device demonstrates the p–n characteristic, and the built-in electric field formed at the two materials' interface contact is beneficial for charge separation. As for sandwich structure, it is usually composed of multiple solid material layers such as light absorption layer, electron transporting material (ETM) and hole transporting material (HTM), or by configuration of combination of solid layer and liquid electrolyte, which is considered effective for charge transport[4−6].

Although these two solar cell structures possess their own advantages for good performance, there still remain challenges in practical working. As a successful example of heterojunction architecture, copper indium gallium selenide(CIGS)-based solar cells offer inherent advantages of efficient carrier separation and collection, and even yield comparable efficiency to Si wafer-based cells[7]. Nevertheless, the interface of the CIGS heterojunction device could also bring about several problems. First, lots of defect states will be introduced into the heterojunction interface, which shall arouse great trap recombination. Second, since there exist band offsets at the CIGS/CdS interface, barrier spikes could possibly form at both the conduction band and valence band site, which will greatly reduce the collection efficiency of the free carriers and lead to relatively low open voltage[8, 9]. As a typical representative of the sandwich architecture, perovskite solar cells, with mixed organic-inorganic halide perovskites ($MAPbX_3$, MA = CH_3NH_3, X = I, Cl, Br) as absorbers, inorganic metal oxides (TiO_2, ZnO, Al_2O_3, etc.) as the ETMs and organic molecules (Spiro-OMeTAD, etc.) as the HTMs, also offer tempting prospects on energy conversion efficiency from less than 5% to over 20% since 2009[10, 11]. But the utilization of the HTM will greatly increase the total cost due to the complex device fabrication process and the difficulty in HTM synthesis. Additionally, the light-induced degradation of the HTM could be a threat to the device stability[12]. To overcome these shortcomings, designing CIGS and perovskite devices with novel structures may be an effective way to enhance the stability and acquire better solar cell performance.

Here, we have designed two novel devices of sandwich CIGS and heterojunction perovskite, referring to the advantages of the architectures of sandwich perovskite (standard) and heterojunction CIGS (standard) solar cells respectively. The similar property of the polycrystalline characteristic and large absorption coefficient of CIGS and perovskite materials makes

* Project supported by the National High-Tech R&D Program of China (No. 2015AA034601), the National Natural Science Foundation of China (Nos. 91333122, 61204064, 51202067, 51372082, 51402106, 11504107), the Ph.D. Programs Foundation of Ministry of Education of China (Nos. 20120036120006, 20130036110012), the Par-Eu Scholars Program, and the Fundamental Research Funds for the Central Universities.
† Corresponding author. Email: mcli@ncepu.edu.cn
Received 23 August 2016, revised manuscript received 10 October 2016

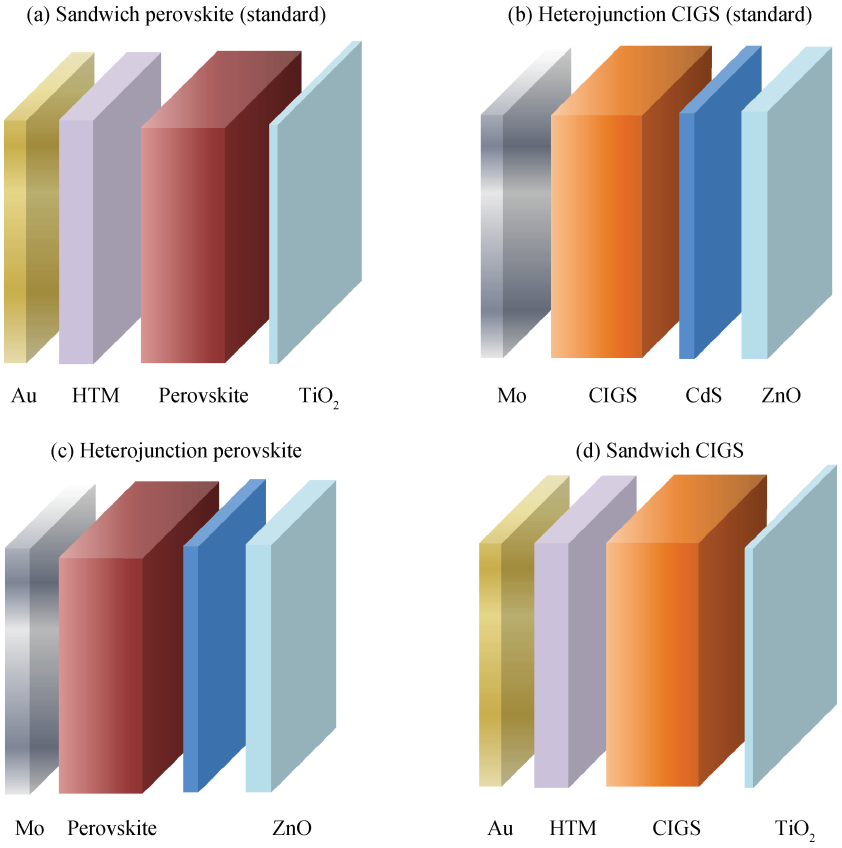

Fig. 1. (Color online) Schematic device structures.

it possible for their architecture reference. The key features of the modulated devices were analyzed by a one-dimensional simulator wxAMPS, which is a new version of the AMPS-1D that is well adapted to modeling various homo-junction, heterojunction, multi-junction solar cells[13–15]. By further varying of the thickness and doping density of absorber layer, we explored their effects on the sandwich CIGS and heterojunction perovskite solar cells' performances.

2. Device simulation parameters

In the wxAMPS simulation, the standard heterojunction CIGS solar cell was in configuration of ZnO/CdS/CIGS, where CIGS is utilized as the p-type absorber layer and ZnO/CdS as the n-type layers, as shown in Fig. 1(b). The standard sandwich perovskite solar cell was in configuration of TiO_2/$MAPbI_3$/Spiro-OMeTAD, as shown in Fig. 1(a). The modulated novel sandwich CIGS and heterojunction perovskite devices were depicted in Figs. 1(d) and 1(c), which are referring to the structures of sandwich perovskite solar cell (Fig. 1(a)) and heterojunction CIGS solar cell (Fig. 1(b)), respectively. Tables 1 and 2 summarize the input modeling parameters for the standard heterojunction CIGS and sandwich perovskite devices, respectively, most of which were selected from recent reported experimental works. For sandwich CIGS and heterojunction perovskite devices, it simply replaced the absorber of the sandwich perovskite device with the CIGS layer and the absorber of the heterojunction CIGS with perovskite device. In our simulation, the AM1.5 solar radiation spectrum was adopted as the light source. Surface recombination rates of both the front and the back were set to 1×10^7 cm/s. Energy levels of defects in the simulated thin film materials were located at the center of their bandgap with the Gaussian-type energetic distribution (characteristic energy 0.1 eV). The absorption coefficients of the CIGS and perovskite layer were derived from Refs. [16, 17], respectively.

3. Results and discussions

Table 3 summarizes the modeling performance parameters of the standard/preliminary modulated CIGS and perovskite solar cells. The preliminary modulated solar cell means the active layer in the modulated structure exhibits the same property as in the original standard structure. For both the standard and sandwich CIGS solar cells, the CIGS layer is set to be 3 μm thick, with doping density equal to 1×10^{16} cm^{-3}; and for both the standard and heterojunction perovskite solar cell, the perovskite layer is set to be 0.35 μm thick, with doping density equal to 1×10^{14} cm^{-3} (intrinsic). However, in terms of the performance values such as the V_{oc}, J_{sc}, FF and PCE values of preliminary modulated devices, they are inferior to the standard devices. Here, we adjusted the thickness and doping density of the active layer of the modulated solar cells to explore their effects on the device characteristics.

When decreasing the thickness of the CIGS layer in the sandwiched one from 3 to 0.35 μm, yet the doping concentration fixed to 1×10^{16} cm^{-3}, there is little change of J_{sc} but V_{oc} is greatly increased (Fig. 2(a)). The value of the efficiency also gets enhanced as a result of the decreased CIGS thickness. Based on this, the doping effect of the absorber layer is further

Table 1. wxAMPS parameters set for the standard perovskite solar cell.

Parameter and unit	Compact TiO_2	$CH_3NH_3PbI_3$	Spiro-OMeTAD
ε_r	100[18]	30[19]	3[20]
E_g (eV)	3.2	1.55[21]	3.17[20]
χ (eV)	4	3.9[22]	2.05[20]
Thickness (μm)	0.03	0.35	0.15
N_a (cm^{-3})	0	0	3×10^{18}
N_d (cm^{-3})	5×10^{19}[18]	0	0
N_c (cm^{-3})	1×10^{21}	2.5×10^{20}[23]	2.8×10^{19}[24]
N_v (cm^{-3})	1×10^{21}	2.5×10^{20}[22]	1×10^{19}[24]

Table 2. wxAMPS parameters set for the standard CIGS solar cell[25].

Parameter and unit	ZnO	CdS	CIGS
ε_r	9	10	13.6
E_g (eV)	3.3	2.4	1.15
χ (eV)	4.4	4.2	4.5
Thickness (μm)	0.2	0.05	3
N_a (cm^{-3})	0	0	2×10^{16}
N_d (cm^{-3})	1×10^{18}	1.1×10^{18}	0
N_c (cm^{-3})	2.2×10^{18}	2.2×10^{18}	2.2×10^{18}
N_v (cm^{-3})	1.8×10^{19}	1.8×10^{19}	1×10^{19}

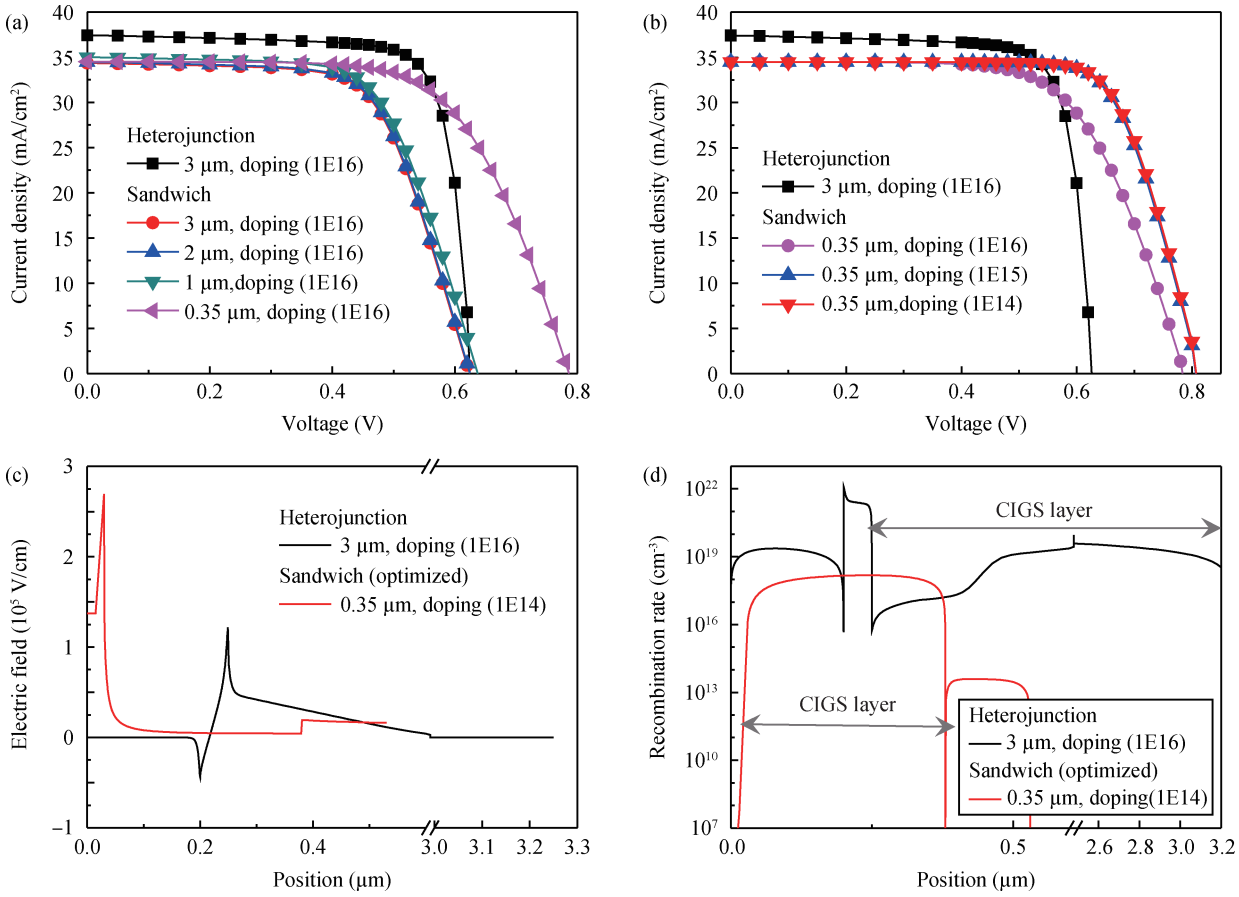

Fig. 2. (Color online) (a) J–V curves of standard/modulated CIGS devices with varied thickness of the absorber layer. The doping is fixed to 1×10^{16} cm^{-3}. (b) J–V curves of standard/modulated CIGS devices with varied doping density of the absorber layer. The thickness in sandwich structures is fixed to 0.35 μm. (c) Electric field, and (d) recombination rate of standard/optimized CIGS devices.

Table 3. Device performances of standard/ preliminary modulated CIGS and perovskite solar cells.

Solar cells		Active layer property	J_{SC} (mA cm^{-2})	V_{OC} (V)	FF (%)	PCE (%)
CIGS	Heterojunction	3 μm, doping (1×10^{16})	37.42	0.63	79.02	18.48
	Sandwich	3 μm, doping (1×10^{16})	34.34	0.62	65.74	14.09
Perovskite	Sandwich	0.35 μm, doping (1×10^{14})	24.08	1.08	76.13	19.71
	Heterojunction	0.35 μm, doping (1×10^{14})	18.24	0.71	73.79	9.6

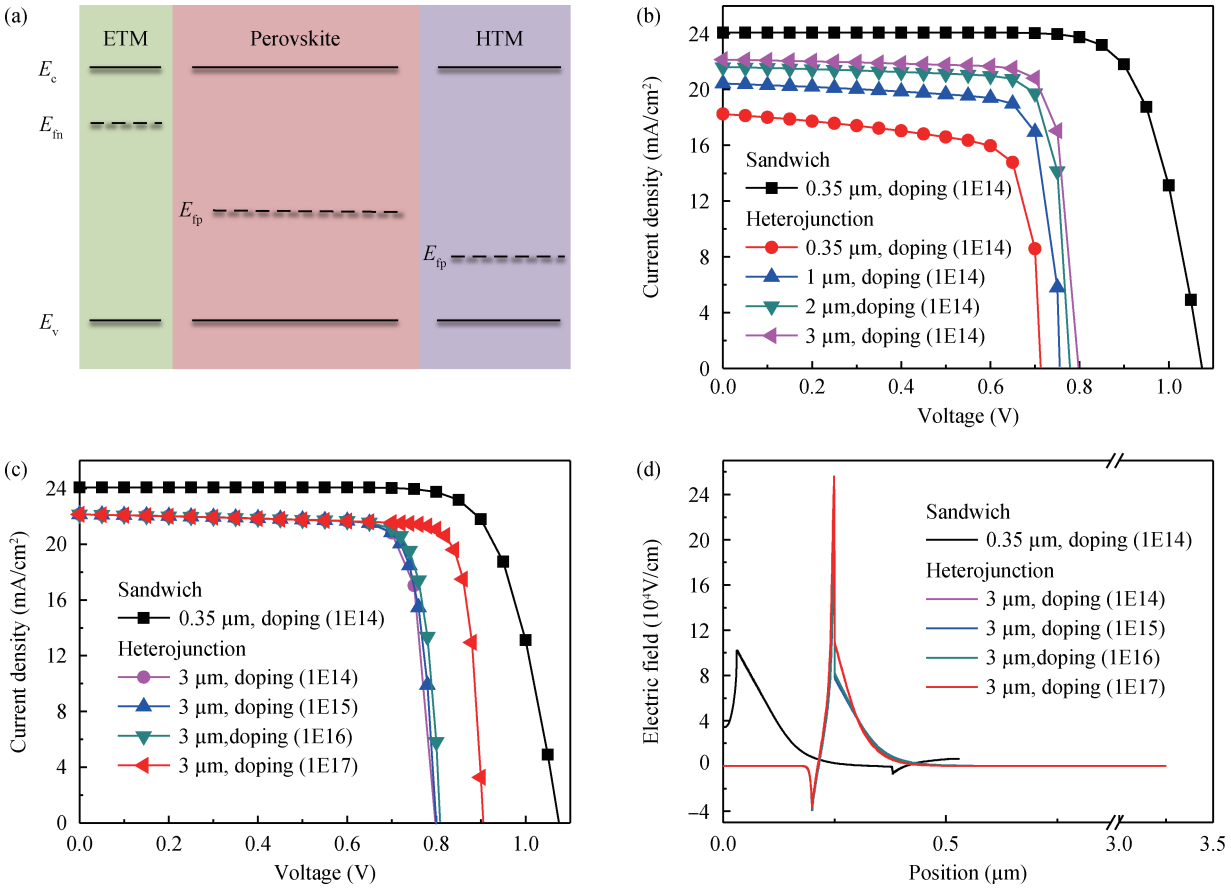

Fig. 3. (Color online) (a) The energy band of the respective layers in perovskite solar cells. (b) J–V curves of standard/modulated perovskite devices with varied thickness of the absorber layer. The doping is fixed to 1×10^{14} cm^{-3}. (c) J–V curves of standard/modulated perovskite devices with varied doping density of the absorber layer. The thickness in heterojunction structure is fixed to 3 μm. (d) Recombination rate distribution in standard/modulated perovskite solar cells.

explored with the thickness fixed to 0.35 μm. It can be seen in Fig. 2(b) that when decreasing the doping density of CIGS layer from 1×10^{16} cm^{-3} to 1×10^{14} cm^{-3}, the device performance improves a lot, especially in the FF and V_{oc} value. An optimized sandwich CIGS device with efficiency of 20.7% is obtained. The reasons for these variations can be explained as follows. Instead of improving the photoelectric property, the addition of p-type HTM even promotes a negative effect on the sandwiched one. This is because the CIGS/HTM interface can provide a weak electric field which is beneficial for hole transporting but also a heterojunction contact which would intensify recombination. Since the span of the interface electric field is much shorter than the width of CIGS layer (3 μm) and there are few carriers generating in the CIGS layer adjacent to CIGS/HTM interface, the electric field originally exploited to separate photo-induced carriers is weak for lack of enough carriers, hence the recombination effect takes the lead. When decreasing the thickness of the CIGS layer in the sandwiched one, although J_{sc} reduces as a result of less light absorption, the built-in electric field could cross the whole active layer and the recombination rate is greatly reduced. Note that V_{oc} depends mainly on the built-in electric field, depletion width and recombination rate, therefore, sandwiched ultra-thin CIGS film leads to rather high V_{oc} and PCE. As doping density decreases, the original n–p–p$^+$ junction gradually turns into n–i–p junction, and CIGS absorption material acts as an i layer. In the i layer, trap-assisted recombination centers are reduced significantly and minority carrier lifetime and diffusion length are longer than in the doped layer, which suppresses the recombination of photon-generated carriers in the CIGS layer. Hence, it is revealed that the sandwich CIGS with thin/intrinsic absorber demonstrates reduced recombination rate (Fig. 2(d)) and broader span of the built-in electric field (Fig. 2(c)) than in standard structure with thick/doped absorber.

When increasing the thickness of the perovskite layer in heterojunction structure from 0.35 μm to 3 μm, yet the doping concentration fixed to 1×10^{14} cm^{-3}, both the J_{sc} and V_{oc} are increased, thus the device efficiency is enhanced accordingly (Fig. 3(b)). This can be ascribed to the more captured sunlight as a result of the thicker absorber thickness. However, the V_{oc} of the heterojunction perovskite device is inferior than in the sandwich structure, which is related to the Fermi levels of the respective layers. In the sandwich device, V_{oc} depends on the difference between the E_{fn} of ETM and the E_{fp} of HTM; in the heterojunction device, V_{oc} depends on the difference between the E_{fn} of ETM and the E_{fp} of perovskite, the smaller difference of the latter leads to low V_{oc}, which is negative for high-efficiency solar cell (Fig. 3(a)). Consequently, to promote the performance of heterojunction structure as much as possible, improving the V_{oc} is of great importance. Here we fix the absorber thickness as 3 μm and further explore the effect of the doping density. As Fig. 3(c) shows, when the doping is less than 1×10^{16} cm^{-3}, there is no evident change of the V_{oc} value, but with the doping density increasing from 1×10^{16} to 1×10^{17} cm^{-3}, the V_{oc} as well as the efficiency gets significantly enhanced. This can be ascribed to the much more efficient charge separation effect induced by the intensified built-in electric field through heavy doping. As Fig. 3(d) shows, when increasing the doping from 1×10^{16} to 1×10^{17} cm^{-3}, the built-in electric field is greatly intensified and even stronger than in the standard sandwich perovskite solar cell, which will enhance the efficiency of the device.

Therefore, for the sandwich CIGS solar cell, the thin/intrinsic CIGS film is more favorable for charge transfer and will lead to better device performance; and for the heterojunction perovskite solar cell, a relatively thick and heavily doped perovskite layer will benefit in promoting its photoelectric property. But since it is hard to fabricate intrinsic CIGS film and there is an interface contact problem in sandwich CIGS, and the thick/doped heterojunction perovskite device could introduce defects induced by pin-holes, it is still a challenge to fabricate the CIGS and perovskite solar cells with novel structures and many works remain to be done to promote their practical application.

4. Conclusion

In this paper, we designed two thin-film polycrystalline solar cells with novel structures: sandwich CIGS and heterojunction perovskite, referring to the advantages of the architectures of sandwich perovskite (standard) and heterojunction CIGS (standard) solar cells, respectively. The characteristics of the devices were investigated by wxAMPS simulation platform with variation of the thickness and doping density of the absorber layers. It is revealed that the sandwich CIGS solar cell with intrinsic/thin CIGS film could lead to better device performance since there is less interface recombination and more efficient charge transfer. The optimized efficiency of sandwich CIGS is 20.7%, much higher than the standard heterojunction CIGS structure (18.48%). The heterojunction perovskite solar cells can be more efficient at employing thick/doped perovskite absorber (16.9%) than these typically utilizing thin and weak-doping/intrinsic perovskite films (9.6%) as a result of the intensified built-in electric field. This structure modulation proves to be useful and can be further applied for other solar cells' design to acquire better performance.

References

[1] Sandberg O J, Sundqvist A, Nyman M, et al. Relating charge transport, contact properties, and recombination to open-circuit voltage in sandwich-type thin-film solar cells. Phys Rev Appl, 2016, 5(4): 044005

[2] Yang Y, Chen W, Dou L T, et al. High-performance multiple-donor bulk heterojunction solar cells. Nat Photonics, 2015, 9(3): 190

[3] Wu Y M, Yang R X, Tian H M, et al. Photoelectric characteristics of $CH_3NH_3PbI_3$/p-Si heterojunction. J Semicond, 2016, 37(5): 053002

[4] Jin H H, Han H J, Lee M H, et al. Stable semi-transparent $CH_3NH_3PbI_3$ planar sandwich solar cells. Energy Environ Sci, 2015, 8(10): 2922

[5] Wu W Q, Lei BX, Rao H S, et al. Hydrothermal fabrication of hierarchically anatase TiO_2 nanowire arrays on FTO glass for dye-sensitized solar cells. Sci Rep, 2013, 3(2): 1352

[6] Sim H, Lee J, Cho S, et al. A study on the band structure of ZnO/CdS heterojunction for CIGS solar-cell application. J Semicond Technol Sci, 2015, 15(2): 267

[7] Contreras M A, Nakada T, Hongo M, et al. ZnO/ZnS(O,OH)/Cu(In,Ga)Se_2Mo solar cell with 18.6% efficiency. Proceedings of World Conference on Photovoltaic Energy Conversion, 2003

[8] Goetzberger A, Knobloch J, Voβ B, et al. The physics of solar cells. Imperial College Press, 2003: 384

[9] Minemoto T, Matsui T, Takakura H, et al. Theoretical analysis of the effect of conduction band offset of window/CIS layers on performance of CIS solar cells using device simulation. Sol Energy Materi Sol Cells, 2001, 67(1–4): 83

[10] http://www.nrel.gov/ncpv/images/efficiency_chart.jpg

[11] Nie W, Tsai H, Asadpour R, et al. High-efficiency solution-processed perovskite solar cells with millimeter-scale grains. Science, 2015, 347(6221): 522

[12] Wei D, Wang T Y, Ji J, et al. Photo-induced degradation of lead halide perovskite solar cells caused by the hole transport layer/metal electrode interface. J Mater Chem A, 2016, 4(5): 1991

[13] Chen W Z, Huang X, Cheng Q J, et al. Simulation analysis of heterojunction ZnO/CdS/Cu(In,Ga)Se_2 thin-film solar cells using wxAMPS. Optik - Int J Light Electron Opt, 2015, 127: 182

[14] Liu Y M, Sun Y, Rockett A. A new simulation software of solar cells-wxAMPS. Sol Energy Mater Sol Cells, 2012, 98(1): 124

[15] Song D D, Wei D, Cui P, et al. Dual function interfacial layer for highly efficient and stable lead halide perovskite solar cells. J Mater Chem A, 2016, 4(16): 6091

[16] https://wiki.cites.illinois.edu/wiki/display/solarcellsim/CIGS

[17] De Wolf S, Holovsky J, Moon S J, et al. Organometallic halide perovskites: sharp optical absorption edge and its relation to photovoltaic performance. J Phys Chem Lett, 2014, 5(6): 1035

[18] Wojciechowski K, Saliba M, Leijtens T, et al. Sub-150 ℃ processed meso-superstructured perovskite solar cells with enhanced efficiency. Energy Environ Sci, 2014, 7(3): 1142

[19] Liu W Q, Zhang Y. Electrical characterization of TiO_2/$CH_3NH_3PbI_3$ heterojunction solar cells. J Mater Chem A, 2014, 2(26): 10244

[20] Snaith H J, Gräzel M. Electron and hole transport through mesoporous TiO_2 infiltrated with spiro-MeOTAD. Adv Mater, 2007, 19(21): 3643

[21] Noh J H, Sang H I, Jin H H, et al. Chemical management for col-

orful, efficient, and stable inorganic-organic hybrid nanostructured solar cells. Nano Lett, 2013, 13(4): 1764

[22] Laban W A, Etgar L. Depleted hole conductor-free lead halide iodide heterojunction solar cells. Energy Environ Sci, 2013, 6(11): 3249

[23] Stoumpos C C, Malliakas C D, Kanatzidis M G. Semiconducting tin and lead iodide perovskites with organic cations: phase transitions, high mobilities, and near-infrared photoluminescent properties. Inorg Chem, 2013, 52(15): 9019

[24] Fonash S J. Solar cell device physics. 2nd Ed. 2010

[25] Liu Y M. Modeling of Cu(In,Ga)Se_2 thin film solar cell device. Nankai University, 2012